

Optimization of Hybrid PZT/Si Electro-optic Phase Modulators.

Gilles F. Feutmba,^{1,2,3} John P. George,^{1,2,3} Koen Alexander^{2,3},
Dries Van Thourhout^{2,3} and Jeroen Beeckman^{1,3}

¹Liquid Crystals and Photonics Group, ELIS Department, Ghent University, Ghent B-9000, Belgium

²Photonics Research Group, INTEC Department, Ghent University-imec, Ghent B-9000, Belgium

³Center for Nano- and Biophotonics (NB-Photonics), Ghent University, Ghent B-9000, Belgium

Pure phase modulators are key building blocks for Photonic Integrated Circuits (PICs). Si modulators based on plasma dispersion suffer from spurious amplitude modulation and high insertion losses. Thin-film electro-optic devices relying on the Pockels effect have therefore been proposed as an ideal alternative for phase modulators on Si. Strongly electro-optic thin films of ferro-electric Lead Zirconate Titanate (PZT) grown on Si waveguides allow for Hybrid PZT/Si phase modulators. We present here simulation studies of a co-planar TE/TM modulator structure.

Introduction

Photonic Integrated Circuits (PICs) are chips in which different optical components (sources, splitters, modulators...) are integrated. Such PICs may offer unprecedented functionality in different application domains such as telecommunication [1], metrology [2], automotive [3], medical [4], Amongst different material platforms, the silicon platform extensively used for electronics is also used for PICs. The well-known silicon (Si) photonic platform allows for small footprint and low-cost PICs. Different optical components such as light sources [5], photodetectors [6,7] and modulators [8,9] have already been demonstrated on this platform. Pure phase modulators are a key building block of these PICs for various applications. Ideally, such a modulator should have a high bandwidth, high modulation efficiency, low loss and should have no spurious amplitude modulation. Si modulators based on plasma dispersion effects (free carrier depletion or accumulation) have high bandwidth and good modulation efficiency but suffer from spurious amplitude modulation and high insertion losses. Electro-optic modulation based on the Pockels effect induce linear refractive index changes as a function of applied electric field and is an ideal way to obtain pure phase modulation. However, due to its centro-symmetric structure, Si does not exhibit the Pockels effect. Thin-film electro-optic devices that possess Pockels effect have therefore been proposed as an alternative for phase modulators on Si. Strongly electro-optic thin films of ferro-electric Lead Zirconate Titanate (PZT) can be grown on Si waveguides by chemical solution deposition [10]. This allows for Hybrid PZT/Si phase modulators. For compact and efficient modulators, the electro-optic overlap in the PZT thin film should be optimized.

Modulator structure and simulation

Different modulator configurations can be designed considering the direction of the crystal/optical of the PZT thin film and the electrode configuration. A co-planar configuration as schemed below is used for this study. The PZT thin films are coated on a lanthanide based intermediate layer [10]. Upon application of an electric field E , the impermeability tensor is expanded in the index notation:

$$\eta_{ij}(E) = \eta_{ij}^{(0)} + r_{ijk}E_k$$

$\eta_{ij}^{(0)}$ is the unperturbed impermeability tensor. The constants r_{ijk} are the Pockels coefficients, which describe the linear electro-optic effect. PZT possesses a 4 mm tetragonal crystal structure with nonzero coefficients r_{33} , r_{13} and r_{51} .

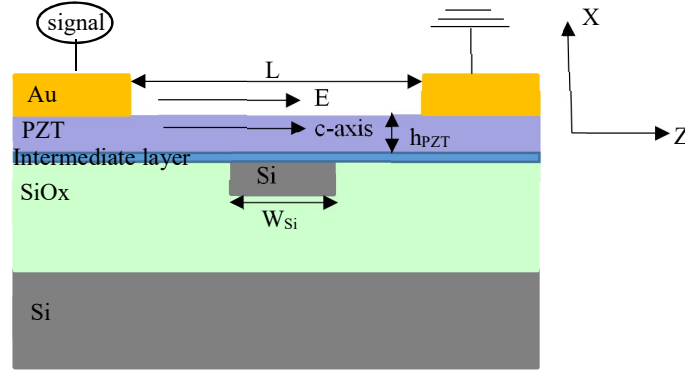


Figure1. The c-axis of the PZT thin film is parallel to the applied field. The electrode spacing (L), width of Si waveguide (W_{Si}) and the PZT thickness (h_{PZT}) are the design parameters investigated.

In the above configuration, the refractive index change along the x and z directions can be expressed as follows

$$n_z = n_e - \frac{n_e^2 r_{33} E}{2}$$

$$n_x = n_o - \frac{n_o^2 r_{13} E}{2}$$

To optimize the performance of the modulator, the electro-optic overlap in the PZT layer has to be maximized. Using COMSOL Multiphysics®, the electrode spacing, PZT thickness and Si waveguide width are varied for an optimum design for both TE and TM phase modulators. A 220 nm thick Si waveguide, 12 nm thick intermediate layer, $r_{33} = 60 \text{ pm/V}$, $r_{13} = 16 \text{ pm/V}$ and ϵ_r (for PZT) = 550 are used for the simulations [11].

Results

The three important figures of merit for phase modulators are the propagation loss α , the tuning efficiency expressed in terms of the voltage-length product $V_\pi L_\pi$ and the $V_\pi L_\pi \cdot \alpha$. The waveguide propagation loss α is calculated as the sum of a contribution caused by the electrodes, and a constant intrinsic propagation loss of 1 dB cm^{-1} . In Fig. 2, $V_\pi L_\pi$ (in units of V.cm) is plotted as a function of Si width and PZT thickness for different electrode spacing for the fundamental TE mode. The electro-optic coupling in the PZT layer increases with thinner Si waveguide, smaller electrode spacing and thicker PZT layer. This leads to a decrease in $V_\pi L_\pi$. Due to the increase in evanescent mode coupling in the PZT layer, the loss due to electrode absorption increases for small electrode spacing and thick PZT (fig. 3 a,d). A trade-off therefore exists between loss and $V_\pi L_\pi$, and an optimum can be found with the product $V_\pi L_\pi \cdot \alpha$ as shown in (fig. 3 c,f) for different Si waveguide widths. A similar conclusion is drawn from TM mode simulations (fig4,5).

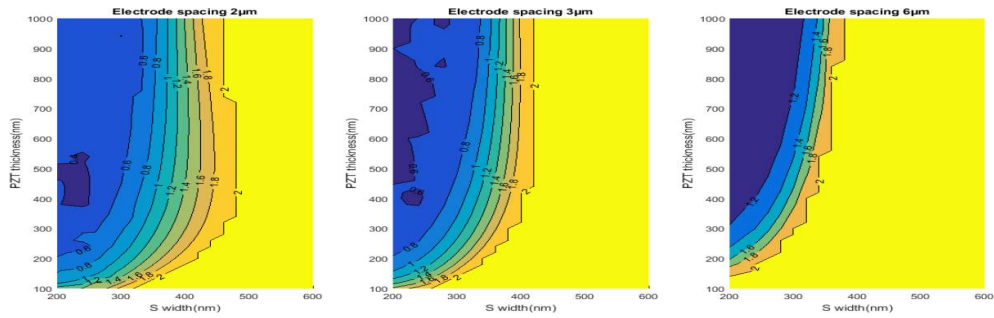


Figure2. TE mode simulations. $V_{\pi}L$ (V.cm) decreases with thinner Si waveguide and thicker PZT due to higher electro-optic overlap in PZT

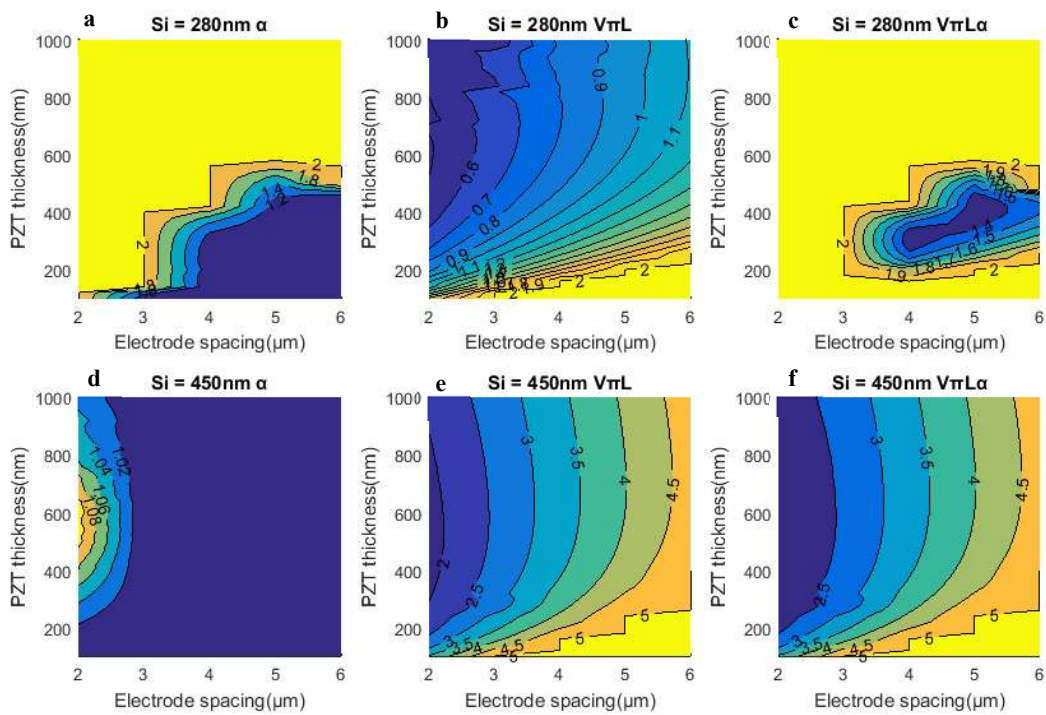


Figure3. TE mode simulations. Simulation of the waveguide loss(dBcm^{-1}) (a, d), the half-wave voltage-length product $V_{\pi}L$ (V.cm) (b, e), and their product $V_{\pi}L\alpha$ (V.dB) (c, f) for Si waveguide widths of 280 nm and 450 nm. An optimum is found at minimum $V_{\pi}L\alpha$.

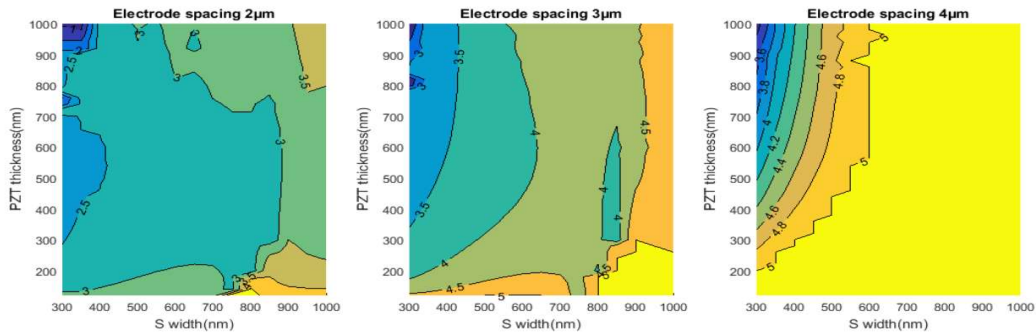


Figure4. TM mode simulations. $V_{\pi}L$ (V.cm) decreases with thinner Si waveguide and thicker PZT due to higher electro-optic overlap in PZT layer

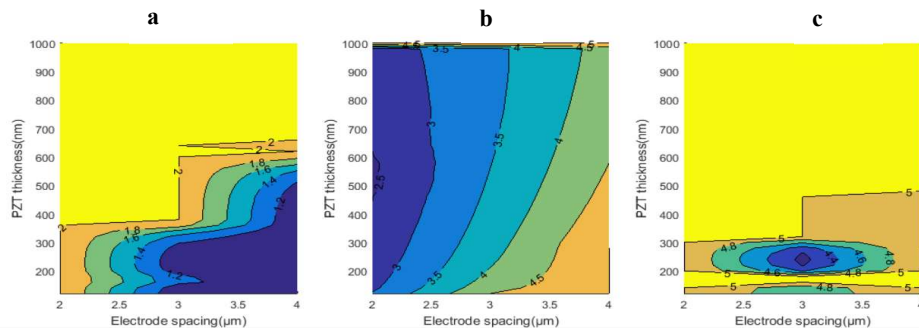


Figure 5. TM mode simulations. Simulation of the waveguide loss α (dBcm⁻¹) (a), the half-wave voltage-length product $V_{\pi}L$ (V.cm) (b), and their product $V_{\pi}L\alpha$ (V.dB) (c) for Si waveguide widths of 300 nm. An optimum is found at minimum $V_{\pi}L\alpha$.

The optimum design for a TE phase modulator, i.e. 280 nm wide Si waveguide, 360 nm thick PZT and 4 μm electrode spacing, gives a $V_{\pi}L_{\pi}$ of 1 V.cm and waveguide loss of less than 2 dB (1,2 dB). For TM modulator, a 300 nm wide Si waveguide, 280 nm thick PZT and 3 μm electrode spacing gives a $V_{\pi}L_{\pi}$ of 3,6 V.cm and waveguide loss of 1.2 dB. These values are better compared to the performance of Si modulators based on plasma dispersion. Also, from a fabrication point of view the designs allow for conventional processing. Although the mode coupling in the PZT for TM is higher than for TE, the large $V_{\pi}L_{\pi}$ obtained for the TM phase modulator is due to the low value of the r_{13} coefficient compared to r_{33} . A transversal configuration (with the c-axis of the PZT film in the x-axis, i.e., r_{51} for the Pockels coefficient) would give better results (lower $V_{\pi}L_{\pi}$ and loss) for both TE and TM. However, such configuration presents fabrication challenges that have to further investigated.

Acknowledgement

Gilles F. Feutmba acknowledges support and funding as an SB-PhD Fellow of the research foundation–Flanders (FWO).

References

- [1] Doerr CR (2015) Silicon photonic integration in telecommunications. *Front. Phys.* 3:37
- [2] C. Koos, et al., "Photonic Integration for Metrology and Sensing," in *Advanced Photonics 2017 (IPR, NOMA, Sensors, Networks, SPPCom, PS)*, OSA Technical Digest (online) paper ITh1A.1.
- [3] Moskowitz, "The Photonics Supply Chain for Autonomous Vehicles - Technology, Tools and Talent," in *Frontiers in Optics 2017*, OSA Technical Digest (online), paper FM2C.1.
- [4] Estevez, M. C., Alvarez, M., & Lechuga, L. M. (2012). Integrated optical devices for lab-on-a-chip biosensing applications. *Laser & Photonics Reviews*, 6(4), 463-487.
- [5] Van Campenhout, Joris, et al. "Electrically pumped InP-based microdisk lasers integrated with a nanophotonic silicon-on-insulator waveguide circuit." *Optics express* 15.11 (2007): 6744-6749
- [6] Michel, et al. "High-performance Ge-on-Si photodetectors." *Nature Photonics* 4.8 (2010): 527.
- [7] Colace, L., et al. "Efficient high-speed near-infrared Ge photodetectors integrated on Si substrates." *Applied physics letters* 76.10 (2000): 1231-1233.
- [8] Reed, Graham T., et al. "Silicon optical modulators." *Nature photonics* 4.8 (2010): 518.
- [9] Liao, Liu, et al. "40 Gbit/s silicon optical modulator for high-speed applications." *Electronics letters* 43.22 (2007): 1196-1197.
- [10] J.P. George, et al. Lanthanide-Assisted Deposition of Strongly Electro-optic PZT Thin Films on Silicon: Toward Integrated Active Nanophotonic Devices, *Acs Appl Mater Inter*, 7 (2015) 13350-13359.
- [11] Alexander, Koen, et al. "Nanophotonic Pockels modulators on a silicon nitride platform." *Nature communications* 9, Article number: 3444 (2018) (2018).